J. Res. Inst. Catalysis, Hokkaido Univ., Vol. 25, No. 3, pp. 175 to 188 (1977)

SCATTERING OF HELIUM AND HYDROGEN MOLECULAR BEAMS FROM THE (111) PLANE OF SILVER

By

Hiromu ASADA*)

(Received December 28, 1977)

Abstract

An experimental study on scattering of He and H_2 molecular beams from Ag (111) surfaces is reported. Spatial distributions of scattered He and H_2, which have been observed both in the incident and transverse planes, consist of a sharp peak of specular reflection and a broad skirt which is clearly distinguished from the former owing to small divergence of the incident beam. The dependence of the broad skirt on the surface temperature, incident angle, incident energy and kind of impinging molecule, is discussed on the basis of coherent inelastic scattering by phonons.

§ 1. Introduction

Scattering of atomic and molecular beams from solid surfaces has been studied in many laboratories.[1~13] In the case of ionic crystal surface,[14~17] such as LiF (001), NaF (001), NaCl (001), and so on, many interesting conclusions have been deduced from accurate observations of diffraction, selective adsorption and thermal diffuse scattering of beams of rare gases and hydrogen atoms and molecules, and lead us to an important understanding of gas-surface interaction potentials and surface lattice vibrations. On the other hand, the nature of metal surfaces is not well understood by means of atomic or molecular beam scattering. One of the reasons for the difficulty is that diffractive scattering of atomic/molecular beams from metal surfaces is not easy to observe except from the strongly corrugated W (112) surface[18,19] or from extremely low temperature surfaces (Ag (111) surface[12,13]). Although thermal diffuse scattering contains a lot of information especially concerning surface lattice dynamics, it is difficult, however, to analyze experimentally both the energy and the momentum transfer between the impinging atom/molecule and the surface, which are

*) Research Institute for Catalysis, Hokkaido University, Sapporo, 060 Japan.

necessary to study the dynamics in detail. But several papers[20~22] have been published on the observation of spatial and/or energy distributions of scattered atoms or molecules, which help us to understand qualitatively the essential features of scattering events.

This paper reports on certain detailed features of spatial distribution of thermal molecular beams of helium and hydrogen scattered from epitaxially grown Ag (111) surfaces, which has been observed both in the incident and transverse planes. In § 2 the molecular beam apparatus constructed for this study and experimental conditions are described. In § 3 the results are discussed qualitatively on the basis of coherent inelastic scattering by phonons.

§ 2. Experimental

2-1. Apparatus

A schematic drawing of the apparatus used in the present study is shown in Fig. 1. It consists of a beam source chamber, an interstage chamber and a scattering chamber. They are differentially pumped by oil-diffusion pumps. The background pressures in the three chambers with the beam generated are 10^{-5}, 10^{-6} and $3\sim10\times10^{-8}$ torr, respectively. The beam is generated by a nozzle made of pyrex glass, whose aperture has an inner diameter $40\sim50\,\mu$m. The position and direction of the nozzle can be

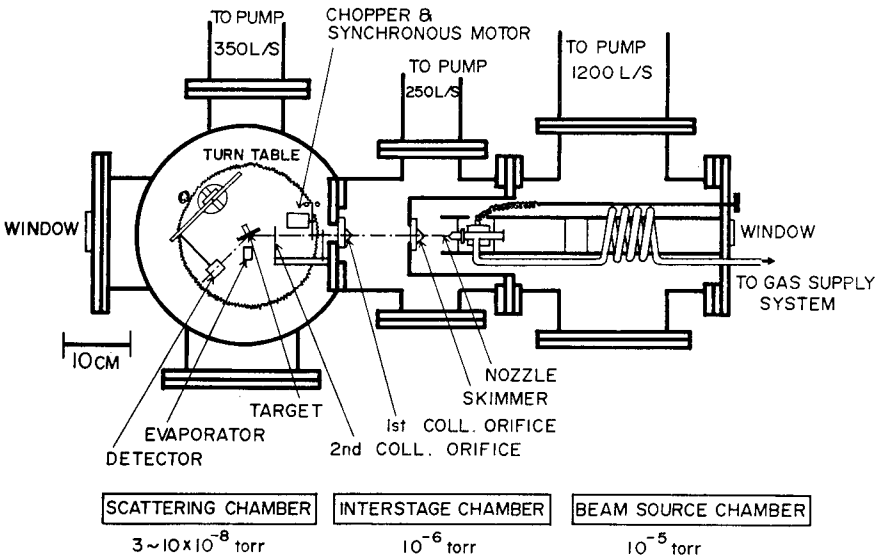

Fig. 1. Experimental apparatus.

adjusted from the outside of the apparatus. The nozzle can also be cooled to *ca.* 150 K by means of a cupper rope whose ends are attached to the nozzle and the bottom of a liquid-N_2 cooled trap, respectively. There is a skimmer of inner diameter 0.62 mm at a distance of 6 to 8 mm from the nozzle. The gas passes through the skimmer, and enters into the interstage chamber as a beam. The beam passes through the first collimating orifice ofinner diameter 1.06 mm to go into the scattering chamber, and after being collimated finally by the second orifice of inner diameter 0.71 mm, collides with a test surface. The flux of the scattered molecules from the test surface is measured by a detector, which is rotated around the surface both in the horizontal and vertical planes. The detector is assembled in a cylindrical stainless steel case of diameter 18 mm and length 30 mm. The principle of detection is to observe an ion current produced by electron-impact ionization of molecules. The output signal from the detector is measured by means of a phase-sensitive detection system since the incident beam is modulated at *ca.* 140 Hz by a chopper wheel. The detector has an angular resolution of about 1.1° with a diameter of the entrance orifice of 1.1 mm and a distance from the test surface of 55 mm. The test surface is located at the center of the scattering chamber, and its direction with respect to the incident beam and its azimuthal angle can be adjusted from the outside.

In Fig. 2 the coodinate system and the definitions of various angles

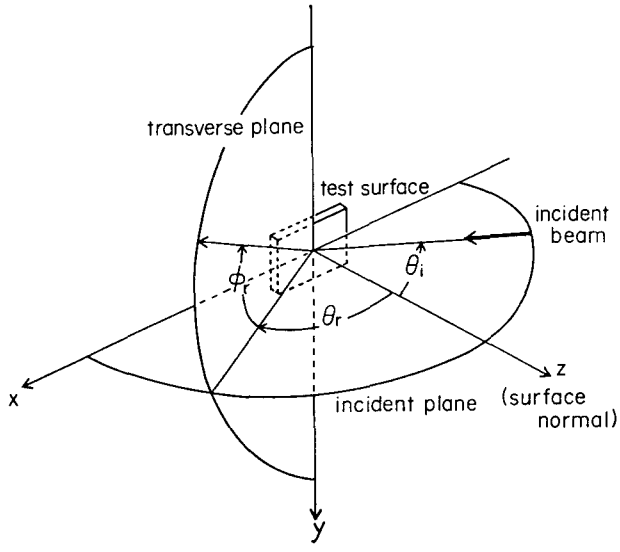

Fig. 2. Definitions of the coordinate system and various angles.

are illustrated. The x and y axes are put on the test surface, and the z axis is the surface normal. The incident angle θ_i is measured from the z axis. The horizontal plane which contains the incident beam and the z axis is called the incident plane. The x axis is defined as the intersection of the incident plane and the surface. The directional vector of scattering makes an angle ϕ_r with the incident plane, and its projection on the incident plane makes an angle θ_r with the z axis. A plane perpendicular to the incident plane is called the transverse plane, and is specified by the angle θ_r.

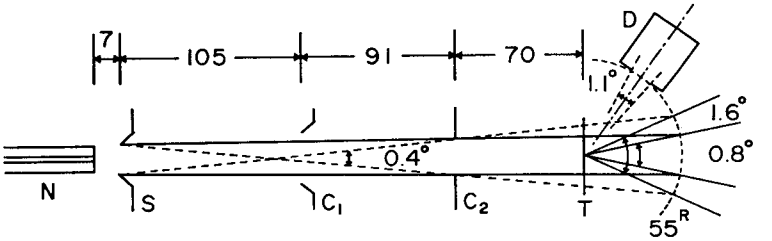

Fig. 3. Geometry of the collimating system. N: nozzle, S: skimmer (0.62 diameter), C_1: 1st collimating orifice (1.06 diameter), C_2: 2nd collimating orifice (0.71 diameter), T: test surface, D: detector, and unit: mm.

2-2. Beams

The geometry of the beam collimation system is represented in Fig. 3. The angular divergence of the incident beam is 0.4°, which is calculated at the periphery of the penumbra. A longitudinal cross section of the incident beam at the position of the test surface has an umbra of diameter 0.74 mm and a penumbra of diameter 1.18 mm. A profile of the direct beam, which is observed downstream along the beam without the surface, is shown in Fig. 4. The full width at half maximum is $0.9\pm0.1°$ in terms of the rotation angle θ_r or ϕ_r of the detector around the test surface.

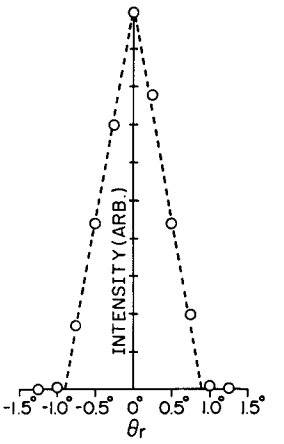

Fig. 4. A profile of the direct beam.

The wave number of the incident beam is determined by observing the $(\bar{1}, \bar{1})$ diffraction of the beam from LiF (001) cleaved surface, whose typical trace is shown in Fig. 5. The peak is broadened due to wave number distribution in the beam. The profile of the $(\bar{1}, \bar{1})$ diffraction peak in the incident plane can be transformed into wave number distribution by the help of Bragg's

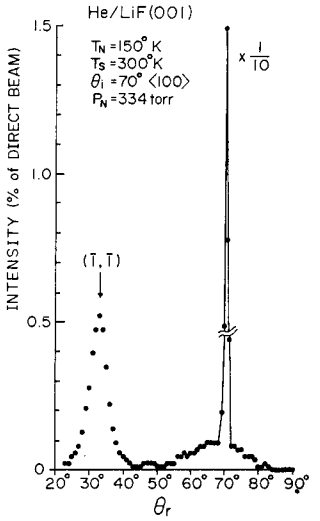

Fig. 5. Diffraction of He beam from LiF (001) surface. nozzle temperature: 150 K, nozzle pressure: 334 torr, and incident angle: 70° along the ⟨100⟩ azimuth. The specular reflection peak is reduced to one tenth. The (1̄, 1̄) diffraction peak can be found at about $\theta_r=33°$.

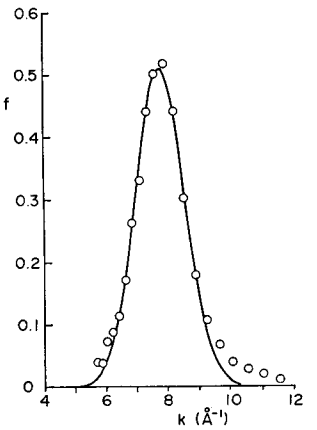

Fig. 6. Wave number distribution transformed from Fig. 5 by use of Eq. (2-1). The solid line is, $f=\text{const}\ k^3 \exp\left[-\left(\frac{k-7.53}{1.13}\right)^2\right]$, obtained by the least square method. The area under the curve is normalized to 1 Å^{-4}.

diffraction condition,

$$k\left(\sin\theta_i-\sin\theta_r\right)=g_{11}\,, \tag{2-1}$$

where k is the wave number of the beam, and g_{11} is 3.13 Å^{-1}, the magnitude of the (1̄, 1̄) surface reciprocal lattice vector. An example of a wave number distribution obtained from Fig. 5 by the transformation is shown in Fig. 6. The wave number distribution, $f(k)$, is well described by the drifted Maxwellian distribution function,[23]

$$f(k)\,dk=\text{const.}\ k^3\exp\left[-(k-k_0)^2/a^2\right]dk\,, \tag{2-2}$$

where k_0 and a are constants. At the tail of higher values of k the observed magnitude is however found a little greater than that expected from Eq. (2-2) (see Fig. 6). The values of the constants k_0 and a, which reproduce the observed distribution best except at its tails of higher and lower k, are evaluated by the least square method at three different incident angles, 50, 60, and 70°. The agreement between the three is very

good. Mean values of k_0 and a are listed in Table 1 with the conditions of the nozzle. Kinetic energy $E_0=(\hbar k_0)^2/2m$, wave length $\lambda_0=2\pi/k_0$, mean wave number $\langle k\rangle$, and mean kinetic energy $\langle E\rangle$, the last two being calculated by the use of Eq. (2-2) and with the obtained values k_0 and a, are also given in the same table.

TABLE 1. Characteristics of the molecular beams

Gas			He		H_2	
Conditions of the nozzle						
temperature	T_N	(K)	300	150	300	150
pressure	P_N	(torr)	462±5	334±5	241±5	163±5
Parameters of wave number distribution and related quantities						
	k_0	(Å^{-1})	9.9 ±0.1	7.5 ±0.1	7.3 ±0.2	5.5 ±0.1
	a	(Å^{-1})	2.3 ±0.1	1.1 ±0.1	1.5 ±0.2	0.6 ±0.1
kinetic energy	E_0	(meV)	51±1	29±1	55±3	31±1
wave length	λ_0	(Å)	0.63±0.01	0.84±0.01	0.86±0.02	1.14±0.01
Mean values						
wave number	$\langle k\rangle$	(Å^{-1})	10.7±0.1	7.7±0.1	7.7±0.2	5.6±0.1
kinetic energy	$\langle E\rangle$	(meV)	61±1	31±1	63±3	33±1

2-3. Test surfaces

Silver surfaces have been prepared by evaporating 99.99% Ag onto cleaved mica surfaces. The holder of the test surface has a heater made of 0.1 mm dia. Pt wire. A 0.1 mm dia. tungsten-constantan thermocouple is attached on the back side of the mica substrate. The thermocouple is calibrated by another one of the same kind attached on an evaporated Ag film by a small amount of SAUEREISEN cement. This procedure permits an accuracy of temperature measurement within an error ±10 K in the range of 450 to 600 K. The deposition of Ag is performed at the substrate temperature 500 to 550 K for 2 to 3 hours at the background pressure $5\sim10\times10^{-8}$ torr. Thereafter the Ag film is annealed at 550 to 600 K for more than 10 min. before scattering experiments. At the end of the experiments, structures of the test surfaces are examined by means of transmission electron diffraction. The films were found to be oriented with ⟨111⟩ axis perpendicular to the surface due to epitaxial growth. Experimental data presented later were obtained on 4 different films, which indicated good reproducibility.

SALTSBURG *et al.*[5] in their similar molecular beam scattering experi-

ments have found no change in the spatial distribution of scattered beams during the deposition of Ag, whose rate exceeds greatly the impinging rate of background gases, and after the deposition has completed. They take this fact as evidence for cleanliness of Ag surfaces used by them. Furthermore, SAU *et al.*[6] have confirmed in their ultra-high vacuum apparatus that silver surfaces are insensitive to background gases.

§ 3. Results and Discussion

3-1. Spatial distributions

Typical traces of spatial distributions of He and H_2 scattered from a Ag surface are shown in Figs. 7 and 8, respectively. In the both cases the surface temperature is 500 K, the incident angle 70°, and the mean kinetic energy *ca.* 30 meV. In each figure, (a) is the distribution in the incident plane, (b) in the transverse plane of $\theta_r=\theta_i=70°$, and (c) in the transverse plane of $\theta_r=65°$ (Fig. 7) or 60° (Fig. 8).

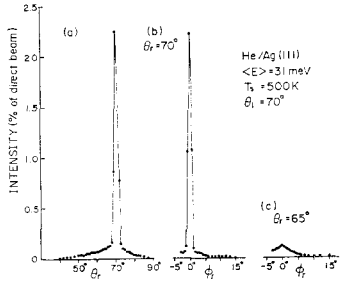

Fig. 7. Spatial distribution of He scattered from Ag (111) surface. $\langle E\rangle=31$ meV, $\theta_i=70°$ and $T_s=$ 500 K. (a) in the incident plane, (b) in the transverse plane of $\theta_r=\theta_i$ and (c) in the transverse plane of $\theta_r=65°$.

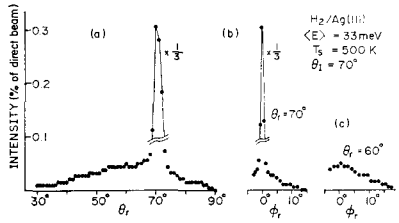

Fig. 8. Spatial distribution of H_2 scattered from Ag (111) surface. $\langle E\rangle=33$ meV, $\theta_i=70°$, and $T_s=$ 500 *K*. (a) in the incident plane, (b) in the transverse plane of $\theta_r=\theta_i$ and (c) in the transverse plane of $\theta_r=60°$. The specular reflection peak is reduced to one third.

The distribution is found to consist of a sharp specular reflection peak and a broad skirt around the former. The broad skirt is regarded as a result of inelastic scattering by phonons of Ag. This inference has been evidenced directly by BISHARA *et al.*[7] and SUBBARAO *et al.*,[9,10] who have observed that the kinetic energy of scattered molecule in the skirt is different from the incident energy, and is supported succesfully by the dependence of the distribution on the surface temperature, incident angle, incident energy and kind of gas molecule, described below.

The observed distribution in the incident plane is qualitatively similar to those of SALTSBURG *et al.*[5] and SUBBARAO *et al.*[8] However the distinction between the specular peak and the broad skirt is clearer than that of SALTSBURG *et al.* SAU *et al.*[6] have observed the distribution on a well-defined Ag (111) surface of single crystal in an ultra-high vacuum system, but it has exhibited a vague pattern, where the specular and the inelastic component are hardly distinguishable from each other. The above difference is thought to come from the angular divergence of the incident beams, which is 2° in the apparatus of SAU *et al.*, 1° in that of SALTSBURG *et al.* and 0.4° at most in the author's. On the other hand, SUBBARAO *et al.*[8] have observed spatial distributions by using a very low energy (several meV) He beam generated by mixing Ar in the beam. The inelastic part of the distribution is found to shift greatly toward the surface normal and to peak at the subspecular region.

The spatial distribution in the transverse planes, shown in (b) and (c) of Figs. 7 and 8, is indicating that the molecules are scattered considerably out of the incident plane. Details of the out-of-plane scattering are illustrated in Fig. 9 for the case of H_2 with $\langle E\rangle = 63$ meV as an example. A trend that the distribution in the transverse plane is more broadened as θ_r decreases, is recognized.

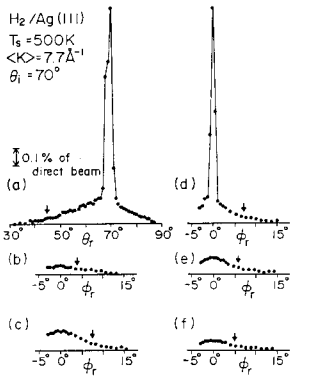

Fig. 9. Spatial distribution of H_2 scattered from Ag (111) surface. $\langle E\rangle = 63$ meV, $\theta_i = 70°$, and $T_s = 500$ K. (a) in the incident plane, (b), (c), (d), (e), and (f), in the transverse plane of $\theta_r = 50$, 60, 70, 75, and 80°, respectively. The arrows in (b)–(f) indicate the positions of ϕ_{max} estimated with $\omega_{max} = 1.31 \times 10^{13}$ sec^{-1}.

The distribution is independent of the azimuthal angle of the surface within the experimental error. Any diffraction spot of the 1st or higher order is not observed, which is compatible with earlier studies.[5~10] But BOATO *et al.*[12] have recently succeeded in observing diffractions of He and H_2 molecular beams from Ag (111) surface cooled to as low as 80 K, and more recently, HORNE *et al.*[13] have reported similar but less precise results with an epitaxially grown Ag (111) surface cooled to 138 K.

3-2. Behavior of inelastic scattering distribution

It is interesting to see in what manner the spatial distribution of inelastic scattering depends on the surface temperature, incident energy or incident angle, since this behavior is related with the mechanism of

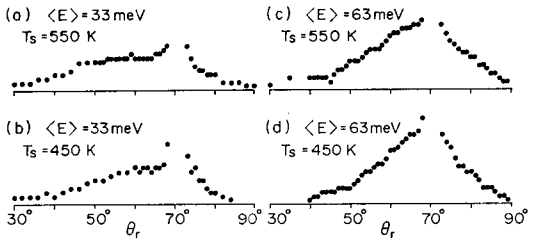

Fig. 10. Dependence of spatial distribution of inelastic scattering of H_2 on the surface temperature. $\theta_i=70°$. The specular peaks are omitted. (a) and (b), $\langle E\rangle=$ 33 meV, $T_s=550$ and 450 K, (c) and (d), $\langle E\rangle=63$ meV, $T_s=550$ and 450 K.

inelastic scattering.

In Fig. 10, the dependence of the distribution on the surface temperature is shown for the case of H_2 beams as an example. Raising the surface temperature from 450 to 550 K, it is found that the scattered intensity increases slightly in the subspecular region (*i. e.* at θ_r lower than θ_i). This fact means that the scattering processes with an energy gain from the surface occur predominantly in the subspecular region.

In Fig. 11 it is illustrated how the distribution changes with the incident energy and the kind of molecule. The difference between He and H_2 in the distribution is not significant, except that it is slightly more intense in the subspecular region in the case of H_2 than He. It is obvious that the distribution becomes broader with a decrease of incident energy, which is in good agreement with earlier studies.[5~8] It is also found that H_2 exhibits broader distribution than He of the same incident energy.

In Fig. 12 the spatial distributions are

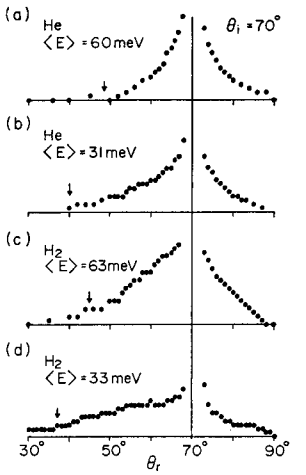

Fig. 11. Spatial distributions of inelastic scattering of four different beams. $\theta_i=70°$ and T_s $=500$ K. The specular peaks are omitted. The arrows indicate the positions of θ_{min} estimated with $\omega_{max}=2.62\times 10^{13}$ sec^{-1}.

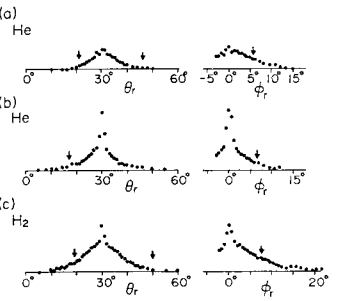

Fig. 12. Spatial distributions in the incident plane and transverse plane of $\theta_r=\theta_i$ in the case of 30° incidence. (a) He with $\langle E\rangle=60$ meV, (b) He with $\langle E\rangle=31$ meV, (c) H_2 with $\langle E\rangle$ $=63$ meV. The arrows in the incident plane indicate the θ_{min} or θ_{max} estimated with $\omega_{max}=2.62\times10^{13}$ sec^{-1}. The arrows in the transverse plane indicate ϕ_{max} estimated with $\omega_{max}=1.13\times10^{13}$ sec^{-1}.

shown in the case of 30° incidence. Comparing with 70° incidence, the distribution changes to have better symmetry around the specular peak. The dependence on the incident energy is less remarkable. It is pointed out again that H_2 gives broader distribution than He of the same incident energy. The spread in the transverse plane is not greatly different from the case of 70° incidence.

3-3. Mechanism of inelastic scattering

Experimental data on scattering of rare gases and hydrogen by metal surfaces have frequently been compared with the hard cube theory[24] based on classical mechanics. The theory has succeeded in interpreting qualitatively the behavior of scattered spatial distributions (*i. e.* the dependence on the surface temperature, incident energy, incident angle and kind of gas molecule). The hard cube theory, as well as other theories[25~27] developed on the basis of one-dimensional collision between the gas molecule and the solid atom, make use of an assumption that the tangential component of momentum of impinging molecule does not change through the scattering processes. But the assumption loses its base owing to the wide spread of the spatial distribution observed in the transverse planes.

Then, a simple discussion is tried from the viewpoint of coherent inelatic scattering by phonons which has been successful in the interpretation of inelastic scattering of He and Ne atoms from ionic crystal surfaces.[20,21]

In the coherent inelastic scattering processes, a tangential component of momentum, as well as total energy, must be conserved in a system composed of the gas molecule and the lattice. Let the magnitudes of momentum of gas molecule before and after scattering be $\hbar\boldsymbol{k}$ and $\hbar\boldsymbol{k}'$, respectively, then the above requirements can be expressed as,

$$k'^2 = k^2 \pm 2m\omega/\hbar\,, \tag{3-1}$$

$$k'_x = k' \cos\phi_r \sin\theta_r = k_x \pm q_x\,, \tag{3-2}$$

$$k'_y = k' \sin\phi_r = \pm q_y\,, \tag{3-3}$$

where $\hbar\omega$ and $\hbar\boldsymbol{q}$ are the energy and momentum of the phonon involved, respectively, and m is the mass of the gas molecule. The upper signs refer to the annihilation, and the lower signs refer to the creation of the phonon. From these relations, a scattering process, where the gas molecule is scattered farthest from the specular angle, is considered in order to estimate the spread of the inelastic spatial distribution. The phonon involved in such a process lies on the boundary of Brillouin zone on the

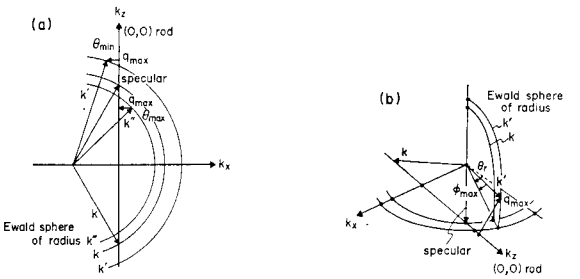

Fig. 13. EWALD's construction in the reciprocal space. (a) scattering processes giving θ_{max} or θ_{min} in the incident plane. The figure roughly corresponds to the situation for H_2 beam with $\langle E\rangle = 63$ meV, $\langle k\rangle = 7.7$ Å^{-1}, and $\theta_i = 30°$. (b) scattering process giving ϕ_{max} in the transverse plane. The q_{max} has no z-component.

xy plane, as indicated in Fig. 13 in the reciprocal space by use of EWALD's construction. The maximum values of ω and q are assumed to be,

$$q_{max} = \pi/b = 1.1 \text{ Å}^{-1},\ \omega_{max} = 2.62 \times 10^{13} \text{ sec}^{-1},$$

where b is the distance, 2.89 Å, between the nearest neighboring atoms on Ag (111) surface. The value of ω_{max} corresponds to a temperature 200 K. The minimum and maximum values, θ_{min} and θ_{max}, of θ_r in the spatial distribution in the incident plane are given by,

$$\sin\theta_{min} = \frac{k_x - q_{max}}{\sqrt{k^2 + 2m\omega_{max}/\hbar}}, \tag{3-4}$$

$$\sin\theta_{max} = \frac{k_x + q_{max}}{\sqrt{k^2 - 2m\omega_{max}/\hbar}}. \tag{3-5}$$

The upper limit ϕ_{max} of ϕ_r is given from

$$\begin{aligned} q_{max}^2 &= q_x^2 + q_y^2 \\ &= -k'^2 \cos^2\theta_r \cos^2\phi_{max} - 2k'k_x \sin\theta_r \cos\phi_{max} + k_x^2 + k'^2. \end{aligned} \tag{3-6}$$

Then,

$$\cos\phi_{max} = \frac{-k_x \sin\theta_r + \sqrt{k_x^2 + (k^2 + 2m\omega_{max}/\hbar - q_{max}^2)\cos^2\theta_r}}{\sqrt{k^2 + 2m\omega_{max}/\hbar}\ \cos^2\theta_r} \tag{3-7}$$

In Fig. 14, the dependence of θ_{max} and θ_{min} on the incident angle is shown. It is found that both θ_{max} and θ_{min} come closer to the specular angle as θ_i decreases. This result is in harmony with the experimental

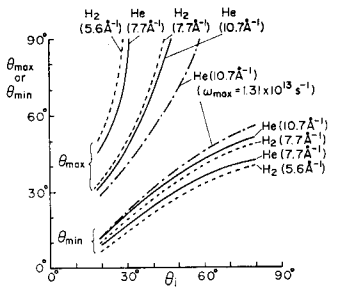

Fig. 14. Dependence of θ_{max} and θ_{min} on θ_i. The designated wave numbers are the mean values $\langle k \rangle$ of the corresponding beams. $q_{max}=1.1$ Å^{-1}, $\omega_{max}=2.62\times10^{13}$ sec^{-1}. Also the case where ω_{max} is reduced to half of the above is illustrated by dotted lines for He of $\langle k \rangle=10.7$ Å^{-1}.

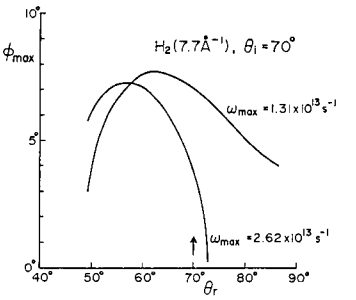

Fig. 15. Dependence of ϕ_{max} on θ_r in the case of H_2 with $\langle k \rangle=7.7$ Å^{-1} and $\theta_i=70°$. Two cases where ω_{max} is equal to 2.62×10^3 sec^{-1} or its half are illustrated.

findings. Also a trend that a higher incident energy gives a narrower distribution and that H_2 gives a broader distribution than He with the same incident energy, coincides with the observed one. The values of θ_{max} and θ_{min} themselves, which are indicated also in Figs. 11 and 12 by arrows, are in good agreement with the observed results. If the value of ω_{max} is reduced to half, the distribution becomes a little narrower, but the value of θ_{min} does not change too much.

In Fig. 15, the dependence of ϕ_{max} on θ_r is shown for the case of H_2 molecular beams with $\langle k \rangle=7.7$ Å^{-1} and $\theta_i=70°$, which should be compared with Fig. 9. The value of ϕ_{max} is considerably dependent on the value of ω_{max}. In the region of large θ_r (approximately speaking, near and larger than the specular angle), the smaller the ω_{max} is, the larger is the ϕ_{max}. This means that the boundary of the distribution in the transverse plane is determined by a vibrational mode with low energy, such as a Rayleigh wave or some transverse waves. When a comparison is made between Figs. 9 and 15, it is found that the lower value of ω_{max} (1.31×10^{13} sec^{-1}) gives better agreement with the observed ones. The corresponding positions of ϕ_{max} are indicated in Figs. 9 and 12 by arrows. The observed spread in the transverse plane is, however, several ten percent greater than that expected.

§ 4. Concluding Remarks

Many theoretical studies[28~30] on molecular beam scattering from solid

surfaces have been reported from the viewpoint of coherent inelastic scattering. Although they are successful in intepreting qualitatively the observed trend, they are not always sufficient quantitatively. In order to obtain a good quantitative agreement it is required to assume a more realistic interaction potential between a gas molecule and a solid atom, but this procedure makes the calculation extremely difficult. Though a direct comparison with the theories has not been made, the simple consideration on the inelastic spatial distribution, described above, has led us to a belief that it should be regarded as a result of coherent inelastic scattering by phonons. It should be emphasized that an accurate and detailed observation of spatial distribution should result in more fruitful insight on the surface lattice dynamics and the gas-surface interation potential.

Acknowledgment

The author wishes to express his sincere thanks to Professor T. TOYA for helpful discussions and encouragement in the course of this work. He also thanks very much Professor T. MATSUI for his advices on experimental techniques and Professor T. NAKAMURA for a critical reading of the manuscript. He is indebted to Mr. T. YAMAZAKI for analyzing the silver samples by transmission electron diffraction, and to Miss A. HIRATSUKA for preparing all of the figures.

References

1) R. E. STICKNEY, *Adv. Atom. Molc. Phys.*, **3**, 143 (1967).
2) J. N. SMITH, JR., Surface Sci., **34**, 613 (1973).
3) J. P. TOENNIES, Appl. Phys., **3**, 91 (1974).
4) S. L. BERNASEK and G. A. SOMORJAI, *Prog. Surface Sci.*, **5**, 377 (1975).
5) H. SALTSBURG and J. N. SMITH, JR., J. Chem. Phys., **45**, 2175 (1966).
6) R. SAU and R. P. MERRILL, Surface Sci., **34**, 268 (1973).
7) M. N. BISHARA and S. S. FISHER, J. Chem. Phys., **52**, 5661 (1970).
8) R. B. SUBBARAO and D. R. MILLER, J. Chem. Phys., **51**, 4679 (1969).
9) R. B. SUBBARAO and D. R. MILLER, J. Vac. Sci. Tech., **9**, 808 (1972).
10) R. B. SUBBARAO and D. R. MILLER, J. Chem. Phys., **58**, 5247 (1973).
11) W. J. HAYS, W. E. RODGERS and E. L. KNUTH, J. Chem. Phys., **56**, 1652 (1972).
12) G. BOATO, P. CANTINI and R. TATAREK, J. Phys., **F 6**, L 237 (1976).
13) J. M. HORNE and D. R. MILLER, Surface Sci., **66**, 365 (1977).
14) D. R. O'KEEFE, J. N. SMITH, JR., R. L. PALMER and H. SALTSBURG, J. Chem. Phys., **52**, 4447 (1970).
15) H. U. FINZEL, H. FRANK, H. HOINKES, M. LUSCHKA, H. NAHR, H. WILSCH and U. WONKA, Surface Sci., **49**, 577 (1975).

16) B. WOOD, B. F. MASON and B. R. WILLIAMS, J. Chem. Phys., **61**, 1435 (1974).
17) G. BOATO, P. CANTINI and L. MATTERA, Surface Sci., **55**, 141 (1976).
18) D. V. TENDULKAR and R. E. STICKNEY, Surface Sci., **27**, 516 (1971).
19) A. G. STOLL, JR., J.-J. EHRHARDT and R. P. MERRILL, J. Chem. Phys., **64**, 34 (1976).
20) B. R. WILLIAMS, J. Chem. Phys., **55**, 3220 (1971).
21) B. F. MASON and B. R. WILLIAMS, J. Chem. Phys., **61**, 2765 (1974).
22) S. S. FISHER and J. R. BLEDSOE, J. Vac. Sci. Tech., **9**, 814 (1971).
23) J. B. ANDERSON and J. B. FENN, Phys. Fluids, **8**, 780 (1965).
24) R. M. LOGAN and R. E. STICKNEY, J. Chem. Phys., **44**, 195 (1966).
25) R. M. LOGAN and J. C. KECK, J. Chem. Phys., **49**, 860 (1968).
26) A. F. DEVONSHIRE, Proc. Roy. Soc., **A 158**, 269 (1937).
27) C. STRACHAN, Proc. Roy. Soc., **A 158**, 591 (1937).
28) E. C. BEDER, *Adv. Atom. Molc. Phys.*, **3**, 205 (1967).
29) J. L. BEEBY, J. Phys., **C 5**, 3438 (1972).
30) N. CABRERA, V. CELLI, F. O. GOODMAN and R. MANSON, Surface Sci., **19**, 67 (1970).